

Corrosion Inhibition Character of Azure B for Mild Steel in Hydrochloric Acid Solution

Shivapura S. Shivakumar, Kikkeri N. Mohana*

Department of Studies in Chemistry, University of Mysore, Manasagangotri, Mysore- 570 006, India

*E-mail: knmsvp@yahoo.com

Received: 16 December 2011 / Accepted: 18 January 2012 / Published: 1 February 2012

The corrosion inhibition behavior of azure B (AB) on mild steel in 0.5 M hydrochloric acid medium was investigated by gravimetric, potentiodynamic polarization and electrochemical impedance measurements. The inhibition efficiency of AB showed an improvement with increasing concentration up to a critical value of AB, beyond this concentration no further effectiveness is observed. The adsorption of AB on mild steel surface was found to obey Langmuir adsorption isotherm. The synergetic effect was also studied between AB and KI, and the addition of KI enhances the inhibition efficiency of AB significantly. Quantum chemical parameters were used to correlate the inhibition efficiency and molecular structure of AB. Further, the surface adsorbed film was analyzed by scanning electron microscopy.

Keywords: Mild steel, acid corrosion, EIS, polarization, adsorption

1. INTRODUCTION

Mild steel is widely used as a constitutional material in many industries due to its good mechanical properties and low cost. The corrosion of mild steel is of fundamental academic and industrial concern that has received a considerable amount of attention especially in hydrochloric acid solution. Several researchers devoted their attention to develop more effective and non-toxic inhibitors to reduce both acid attack and protection aspects [1-3]. Acid pickling baths are employed to remove undesirable scale from the surface of the metals. Once the scale is removed, the acid is then free for further attack on the metal surface. Hence, several organic compounds containing N, O and S have been studied as corrosion inhibitors by several authors [4, 5]. The use of organic compounds with hetero atoms based corrosion inhibitors is often associated with chemical and/or physical adsorption, involving a variation in the charge of adsorbed substance and a transfer of charge from one phase to the other [6]. Special attention was paid to the effect of electron donating atom and electron

withdrawing groups which are responsible for adsorption and hence on the performance [7]. Furthermore, it has been observed that the adsorption mainly depends on steric factor, aromaticity and structural properties of the organic compounds, which induce greater adsorption of the inhibitor molecules onto the surface of the metal [8, 9].

Synergistic corrosion inhibitor plays an important role both in theoretical and practical research [10]. Corrosion inhibition synergism takes place due to ion-pair interaction between organic cation and anion. Synergism between organic inhibitors and halide ions in metal corrosion has been investigated by many researchers [10-12]. Synergistic inhibition effects of organic inhibitor/metallic ion mixture [13] and organic inhibitors/organic inhibitor mixture [14] on the corrosion metal in acid media have also been reported.

Dyes have been used as effective corrosion inhibitors in acid medium because they possess molecular structure recommended for investigation as possible corrosion inhibitor [15-17]. Azure B is a water soluble thiazin dye formed by the oxidation of methylene blue. It is strongly metachromatic (one dye exhibiting two different color reactions), and is used in making azure eosin stain for blood smear staining.

In the present investigation, the inhibitive performance of AB on mild steel in 0.5 M HCl at different temperatures have been studied by gravimetric, potentiodynamic polarization and electrochemical impedance techniques. The inhibition mechanism has been discussed on the basis of molecular properties such as dipole moment, energies of the highest occupied (E_{HOMO}) and lowest unoccupied (E_{LUMO}) molecular orbitals and Mulliken charges. The present work was also designed to understand the effect of synergistic inhibition between AB and I^- ions on the corrosion of mild steel in HCl medium.

2. EXPERIMENTAL

2.1. Materials and test solutions

Mild steel coupons containing (in wt%) 0.016 P, 0.322 Si, 0.01 Al, 0.062 Cr, 0.05 Mn, 0.09 C, 0.05 S and balance iron were used for electrochemical and gravimetric studies. Mild steel coupons were mechanically polished on silicon carbide papers (400, 600, 1000, and 1200), washed with double-distilled water, degreased in ethanol, and finally dried at room temperature before being immersed in the acid solution.

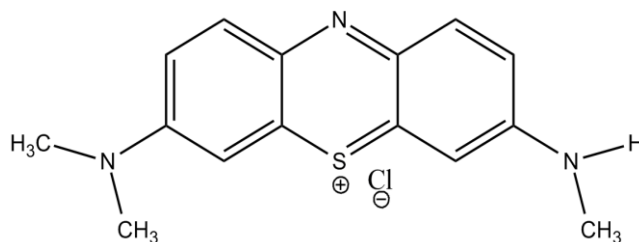


Figure 1. Chemical structure of AB.

The aggressive solution was prepared by dilution of analytical grade HCl. *Azure B (AB)*, (3-Methylamino-7-dimethylaminophenothiazin-5-ium chloride) was procured from Sigma Aldrich and used without further purification. The chemical structure of AB is shown in Fig. 1. A stock solution of AB (10 mM) was prepared by weighing an appropriate amount of it and dissolved in 0.5 M HCl, and series of concentrations (0.5 mM – 5 mM) were prepared from this stock solution.

The KI used was obtained from Merck and a stock solution of 20 mM was prepared by weighing an appropriate amount of the salt and dissolved in 0.5 M HCl. All other chemicals used were analytical grades of purity.

2.2. Gravimetric measurements

A gravimetric experiment was carried out in a glass cell and the solution volume was 100 cm³. The temperature of the environment was maintained by thermostatically controlled water bath (Weiber, India) with an accuracy of ± 0.2 °C under aerated condition. The mild steel specimens used were rectangular with a dimension of 1 cm \times 1 cm \times 0.3 cm. The initial weight of the specimen was recorded by using an analytical balance (precision ± 0.1 mg). After the corrosion test in 0.5 M HCl with and without inhibitor, the specimens were carefully washed in double distilled water, dried and then weighted. The weight loss of specimen was determined after an immersion period of 6 h. Triplicate experiments were performed in each case, and the mean value of the corrosion rate was reported and expressed in mg cm⁻² h⁻¹.

2.3. Electrochemical measurements

Electrochemical measurements were carried out in a conventional three-electrode glass cell with a platinum counter electrode and a saturated calomel electrode (SCE) as reference. All tests were performed in continuously stirred conditions at 303 K by using CHI660D electrochemical workstation. The mild steel electrode was maintained at open circuit conditions for 1 h and thereafter anodic and cathodic polarization curves were recorded in the potential range from -900 to +500 mV with a scan rate of 0.4 mV s⁻¹. The AC impedance measurements were performed in the frequency range from 10 kHz to 0.05Hz with signal amplitude of ± 10 mV.

3. RESULTS AND DISCUSSION

3.1. Weight loss measurement

The weight loss measurements were carried out as a function of temperature (30 - 60 °C) and concentration (1-5 mM) at 6 h immersion time. The percentage inhibition efficiencies (IE %) and corrosion rates (C_R) are summarized in Table 1.

The percentage inhibition efficiency was calculated using the following equation:

$$IE(\%) = \frac{(C_R)_a - (C_R)_p}{(C_R)_a} \times 100 \tag{1}$$

where, $(C_R)_a$ and $(C_R)_p$ are the corrosion rates in the absence and presence of inhibitor, respectively.

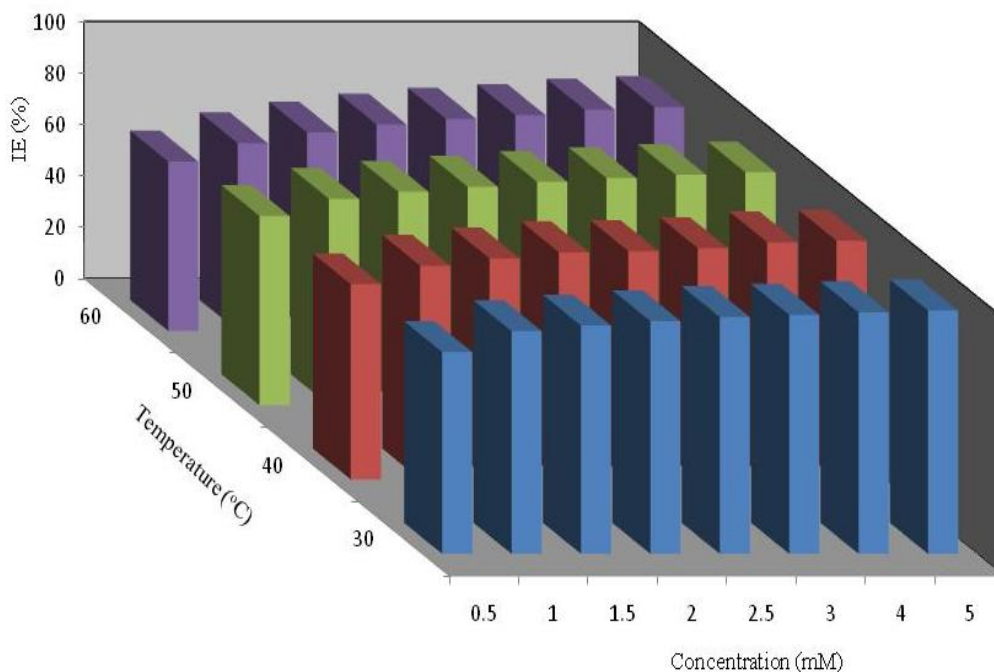


Figure 2. Variation of IE (%) as a function of temperature and concentration of AB.

Table 1. C_R and IE (%) obtained from weight loss measurements of mild steel in 0.5 M HCl containing various concentrations of AB at different temperatures

C, mM	Temperature							
	30 °C		40 °C		50 °C		60 °C	
	C_R , $\text{mg cm}^{-2} \text{h}^{-1}$	IE (%)	C_R , $\text{mg cm}^{-2} \text{h}^{-1}$	IE (%)	C_R , $\text{mg cm}^{-2} \text{h}^{-1}$	IE (%)	C_R , $\text{mg cm}^{-2} \text{h}^{-1}$	IE (%)
0	1.394	-	1.898	-	2.628	-	3.351	-
0.5	0.314	78.55	0.485	76.03	0.782	73.67	1.212	65.92
1.0	0.185	86.73	0.318	83.25	0.517	80.33	0.902	73.08
1.5	0.155	88.88	0.265	86.04	0.443	83.14	0.763	77.23
2.0	0.131	90.60	0.219	88.46	0.393	85.05	0.658	80.36
2.5	0.109	92.18	0.210	88.94	0.342	86.99	0.665	82.60
3.0	0.097	93.04	0.189	90.04	0.305	88.39	0.583	84.04
4.0	0.084	94.05	0.145	92.36	0.271	89.69	0.465	86.12
5.0	0.073	94.76	0.120	92.94	0.238	90.68	0.432	87.11

The variation of inhibition efficiency with temperature and inhibitor concentration is shown in Fig. 2. It is obvious from the figure that AB inhibit the corrosion of mild steel in 0.5 M HCl solution at

all concentrations used in this study. The inhibition efficiency was seen to increase with increasing inhibitor concentration up to an optimum level after which there is no remarkable change in the inhibition efficiency. The inhibitor was found to attain the maximum inhibition efficiency at 5 mM concentration.

3.2. Potentiodynamic polarization

Table 2. E_{corr} , I_{corr} , R_{ct} and IE (%) obtained from polarization and impedance measurements for mild steel in 0.5 M HCl containing various concentrations of AB at 30 °C

C, mM	EIS		Polarization		
	R_{ct} , $\Omega\text{ cm}^2$	IE (%)	E_{corr} , mV	I_{corr} , mA cm^{-2}	IE (%)
0	18.4	-	-513	4.840	-
0.5	78.0	76.38	-487	1.155	76.14
1.0	110.5	83.33	-468	0.720	85.13
1.5	210.2	91.24	-461	0.396	91.82
2.0	246.2	92.52	-456	0.387	92.01
2.5	299.8	93.86	-451	0.346	92.84
3.0	315.3	94.16	-448	0.316	93.47
4.0	368.9	95.01	-445	0.209	95.68
5.0	371.1	95.04	-443	0.202	95.83

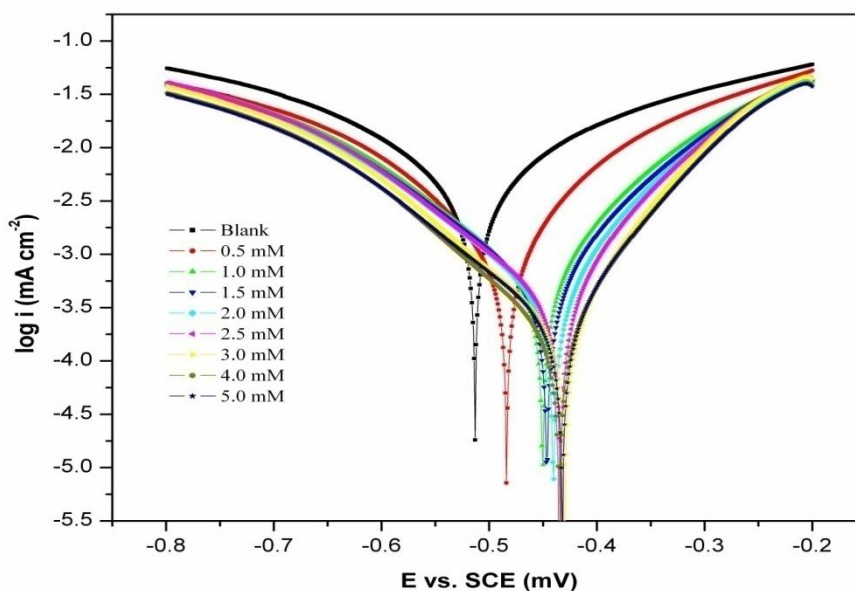


Figure 3. Polarization curves for mild steel in 0.5 M HCl at various concentrations of AB at 30 °C, and at a scan rate of 0.42 mV s^{-1} .

Polarization behavior of mild steel in 0.5 M HCl without and with different concentration of AB is shown in Fig. 3, and various electrochemical parameters such as corrosion potential (E_{corr}),

corrosion current density (I_{corr}), percentage inhibition efficiency obtained from cathodic and anodic curves are given in Table 2. The IE (%) and degree of surface coverage (θ) values were calculated from the following equation:

$$IE (\%) = \frac{(I_{corr})_a - (I_{corr})_p}{(I_{corr})_a} \times 100 \tag{2}$$

where, $(I_{corr})_a$ and $(I_{corr})_p$ are the corrosion current density (mA cm^{-2}) in the absence and presence of the inhibitor, respectively. From the Fig. 3, it is clearly seen that AB shifted both anodic and cathodic branches of polarization curves to lower values of current density indicating AB acts as mixed type of inhibitor. That is addition of AB to HCl solution reduces the anodic dissolution of mild steel and also retards the cathodic hydrogen evolution reaction [18]. The corrosion potential (E_{corr}) shifted slightly to more positive values and I_{corr} decreased when the concentration of AB was increased. The inhibiting effect of AB may be due to the increase in blocked fraction of the electrode surface by adsorption and formation of a barrier film on the electrode surface [19].

3.3. Electrochemical impedance technique

The corrosion behavior of mild steel in 0.5 M HCl in the absence and presence AB was investigated by the electrochemical impedance technique over the frequency range from 10 kHz to 0.01 Hz at 30 °C and results are shown in Fig. 4 and Table 2.

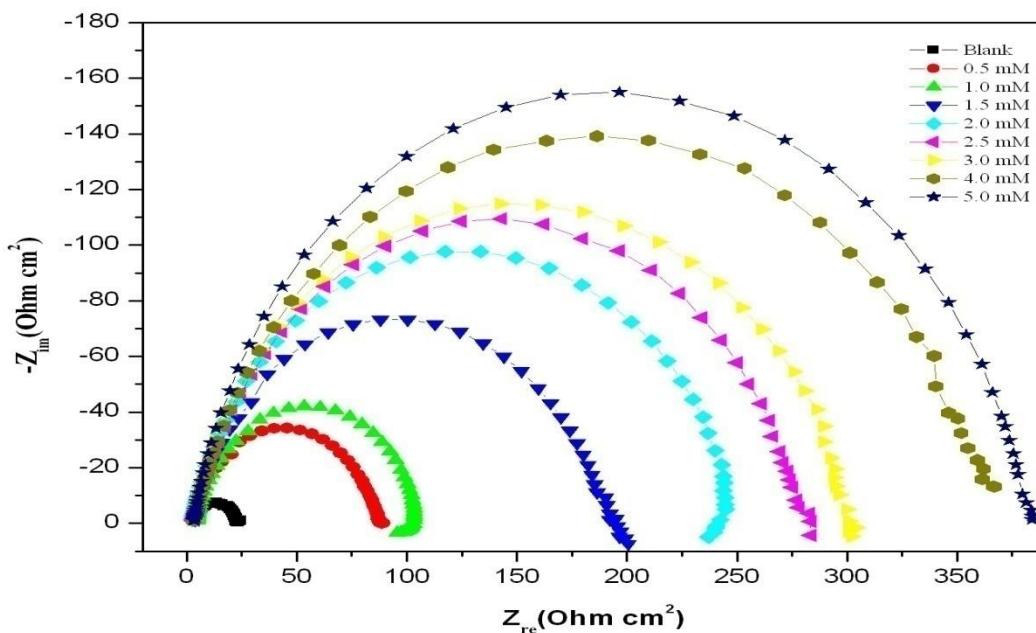


Figure 4. Nyquist plots for mild steel in 0.5 M HCl in the absence and presence of various concentration of AB at 30 °C.

The simple equivalent Randle circuit is shown in Fig. 5 which includes the solution resistance (R_s), charge transfer resistance (R_{ct}) and double layer capacitance (C_{dl}). The inhibition efficiency IE (%) was calculated using the charge transfer resistance as follows:

$$IE(\%) = \frac{(1/R_{ct})_a - (1/R_{ct})_p}{(1/R_{ct})_a} \times 100 \quad (3)$$

where $R_{ct(a)}$ and $R_{ct(p)}$ are the charge transfer resistance in the absence and presence of inhibitor, respectively.

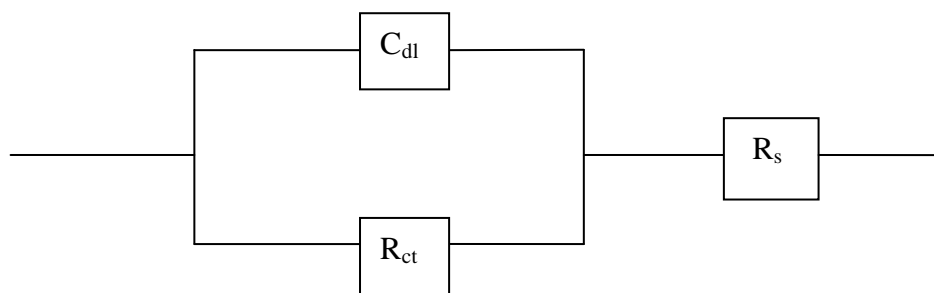


Figure 5. Equivalent circuit diagram.

The Nyquist plots containing depressed semi-circle, whose size increases with the inhibitor concentration represents a charge transfer process mainly controlling the corrosion of mild steel. It is evident from these plots that the impedance response of mild steel in uninhibited acid solution has significantly changed after the addition of the inhibitor in the aggressive solution. The R_{ct} values increased with the increasing concentration of the inhibitor indicating that more inhibitor molecule adsorb on the metal surface at higher concentration and form a protective film on the metal–solution interface [20, 21]. On the other hand, the value of C_{dl} decreased with increasing inhibitor concentration. Decrease of C_{dl} may be caused by a reduction in local dielectric constant and/or by an increase in the thickness of the electrical double layer. These results indicate that the inhibitor molecules act by adsorption on the metal/solution interface [22, 23]. These observations suggest that AB molecule function by adsorption at the metal surface and thereby causing a decrease in the C_{dl} values and an increase in the R_{ct} values.

3.4. Effect of temperature

In order to investigate the stability of the adsorbed layer of inhibitor on mild steel surface and to evaluate the activation parameters of the corrosion process, weight loss measurements were carried out in the temperature range of 303–333 K in the absence and presence of different concentration of AB during 6 h immersion time. Results thus obtained are shown in Fig. 2. It is evident from Fig. 2 that the inhibition efficiency of AB is inversely proportional to temperature. This is due to increased rate of

dissolution process of mild steel and partial desorption of the inhibitor from the metal surface with temperature [24]. The dependence of corrosion rate on temperature can be expressed by the following Arrhenius and transition state equations:

$$C_R = A \exp\left(-\frac{E_a^*}{RT}\right) \tag{4}$$

$$C_R = \frac{RT}{Nh} \exp\frac{\Delta S^*}{R} \exp\left(-\frac{\Delta H^*}{RT}\right) \tag{5}$$

where E_a^* , the apparent activation energy, A the pre-exponential factor, ΔH^* the apparent enthalpy of activation, ΔS^* the apparent entropy of activation, h Planck's constant and N the Avogadro number, respectively.

Table 3. Activation parameters for mild steel in 0.5 M HCl in the absence and presence of different concentrations of AB

C, mM	E_a^* , kJ mol ⁻¹	k	ΔH^* , kJ mol ⁻¹	$\Delta H = E_a^* - RT$, kJ mol ⁻¹	ΔS^* , J mol ⁻¹ K ⁻¹
0	24.82	26370	22.18	21.97	-169.06
0.5	37.17	1077334	35.33	34.32	-138.22
1.0	43.91	6783475	41.27	41.05	-122.96
1.5	44.39	6851650	41.74	41.54	-122.87
2.0	45.49	8886111	42.85	42.64	-120.70
2.5	46.33	10745526	43.97	43.47	-118.16
3.0	47.02	12609991	44.37	44.16	-117.80
4.0	48.59	19191922	45.95	45.74	-114.32
5.0	50.40	33598769	47.76	47.55	-109.66

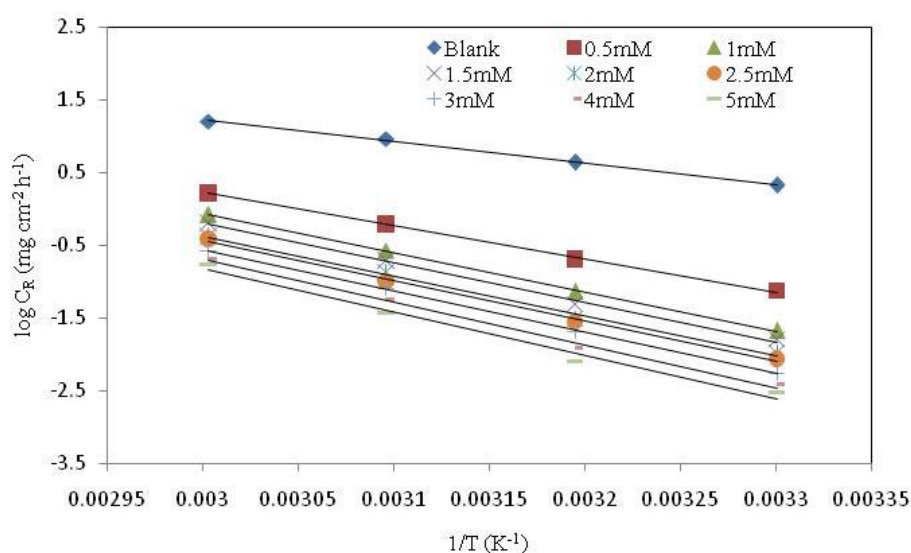


Figure 6. Arrhenius plots for mild steel in 0.5 M HCl in the absence and presence of different concentrations of AB.

The apparent activation energy and pre-exponential factor for a wide range of concentration of AB was calculated from a plot of logarithm of C_R versus $1/T$ (Fig. 6) and the results are shown in Table 3. All the linear regression coefficients are close to unity, indicating that dissolution of mild steel in hydrochloric acid can be explained using the kinetic model. The values of E_a^* and k at various concentrations of AB are computed from slopes and intercepts, respectively. Inspection of Table 3 showed that, activation energy increased in inhibited acid compared to the free acid. The increase in E_a^* could be interpreted as physisorption or columbic type of adsorption and appreciable decrease in the adsorption of the inhibitor on the surface of mild steel with increasing temperature [25, 26].

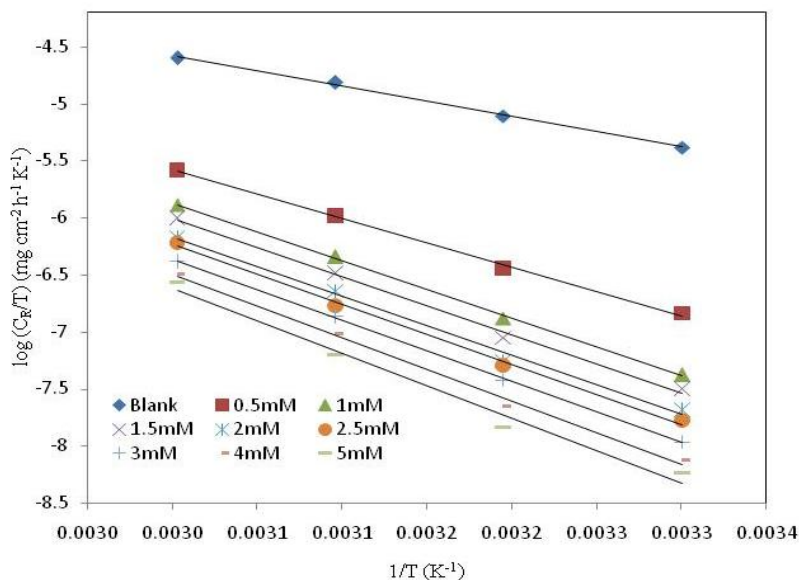


Figure 7. Alternative Arrhenius plots for mild steel dissolution in 0.5 M HCl in the absence and presence of different concentrations of AB.

Further, using Eq. (5), plots of $\log(C_R/T)$ versus $1/T$ gave straight lines (Fig. 7) with a slope of $(-\Delta H^*/2.303R)$ and an intercept of $[\log(R/Nh) + \Delta S^*/2.303R]$, from which the values of ΔH^* and ΔS^* were calculated and are summarized in Table 3. The positive sign of the activation enthalpy (ΔH^*) reflects the endothermic nature of the steel dissolution process and that the dissolution of steel is difficult. The entropy of activation decreased in the presence of AB compared to free acid. Such variation reflects the formation of an ordered stable film of inhibitor on the mild steel surface [27, 28]. Investigation of Table 3 revealed that the activated complex in the rate determining step represent an association rather than a dissociation step, meaning that a decrease in disordering takes place on moving from reactants to the activated complex [29, 30].

3.5 Adsorption isotherm

Organic inhibitors inhibit the corrosion by adsorption onto the metal surface. It depends on the nature as well as the surface charge of the metal, the adsorption mode, its chemical structure and the type of the aggressive solution [31].

Table 4. Thermodynamic parameters for adsorption of AB on mild steel in 0.5 M HCl at different temperatures from Langmuir adsorption isotherm

Temperature, K	R ²	K _{ads} , L mol ⁻¹	ΔG _{ads} , kJ mol ⁻¹	ΔH _{ads} , kJ mol ⁻¹	ΔS _{ads} , J mol ⁻¹ K ⁻¹
303	0.986	11250.9	-33.62		
313	0.988	10441.4	-34.56	-6.74 ^a	88.80 ^a
323	0.993	9986.15	-35.51	-7.15 ^b	87.00 ^b
333	0.990	8725.71	-36.22		

^a values obtained from Eq. (8)

^b values obtained from Eq. (9)

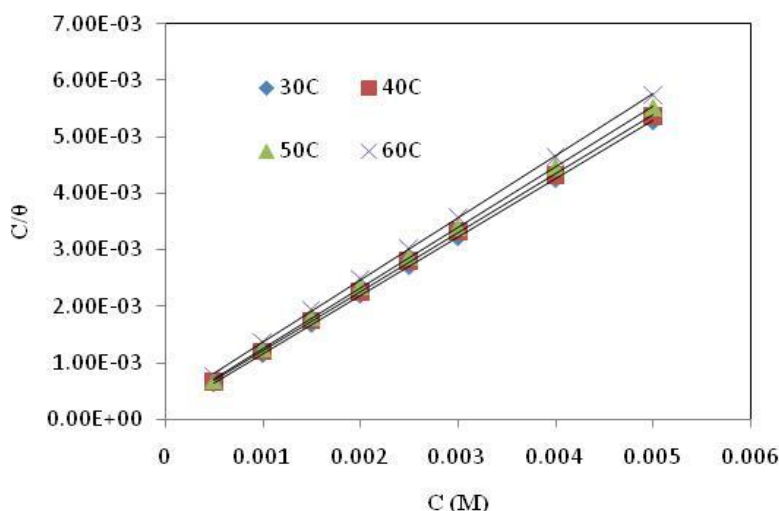


Figure 8. Langmuir adsorption isotherm of AB on mild steel in 0.5 M HCl at different temperatures.

In order to get a better understanding of the adsorption mode of the inhibitor on the metal surface, the data were tested graphically by fitting it to various isotherms to find the best isotherm which describes this study. The value of correlation coefficient (R²) was used to determine the best fit isotherm. Langmuir adsorption isotherm was found to fit well with the experimental data. According to this isotherm, θ is related to the C and adsorption equilibrium constant K_{ads}, via the following equation:

$$\frac{C}{\theta} = \frac{1}{K_{ads}} + C \tag{6}$$

Using Eq. 6, plots of log (C/θ) versus C gave straight lines (Fig. 8) with a slope of around unity confirming that the adsorption of AB on mild steel surface in hydrochloric acid solution obeys the Langmuir adsorption isotherm. The values of Langmuir adsorption parameters obtained from the plots are recorded in Table 4. The results shows that the slopes and R² values are very close to unity indicating strong adherence of the adsorbed inhibitors to the assumptions of Langmuir [32]. The equilibrium constant of adsorption obtained from the slopes of the Langmuir isotherms were used to calculate the free energy for the adsorption AB on the surface of mild steel. The free energy of

adsorption of AB on the metal surface is related to the equilibrium constant of adsorption according to equation (7).

$$K_{ads} = \frac{1}{55.5} \exp\left(\frac{-\Delta G_{ads}}{RT}\right) \quad (7)$$

where R is the universal gas constant, T is the absolute temperature, ΔG_{ads} is the free energy of adsorption and 55.5 is the concentration of water in solution (mol L^{-1}).

The enthalpy and entropy of adsorption (ΔH_{ads} and ΔS_{ads}) can be calculated using the equation (8)

$$\ln K_{ads} = \ln \frac{1}{55.5} - \frac{\Delta H_{ads}}{RT} + \frac{\Delta S_{ads}}{R} \quad (8)$$

Using Eq. (8), the values of ΔH_{ads} and ΔS_{ads} were evaluated from the slope and intercept of the plot of $\ln K_{ads}$ versus $1/T$ (Fig. 9).

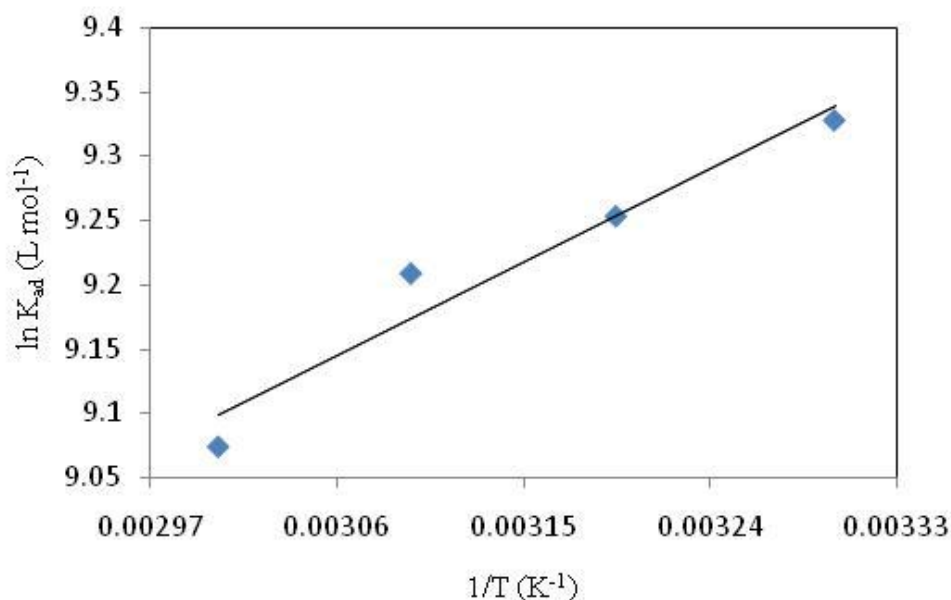


Figure 9. Plot of $\ln K_{ads}$ versus $1/T$.

The values of ΔG_{ads} , ΔH_{ads} and ΔS_{ads} are listed in Table 4. From the results, it is significant to note that the calculated values of ΔG_{ads} are negative which indicate that adsorption is a spontaneous process. Generally, the values of ΔG_{ads} around -20 kJ mol^{-1} or lower are consistent with the electrostatic interaction between charged molecules and the charged metal surface (physisorption) while those around -40 kJ mol^{-1} or more negative involve chemisorption [33]. In the present study, the value of ΔG_{ads} is about -35 kJ mol^{-1} , which probably means that both physisorption and chemisorption are taking place.

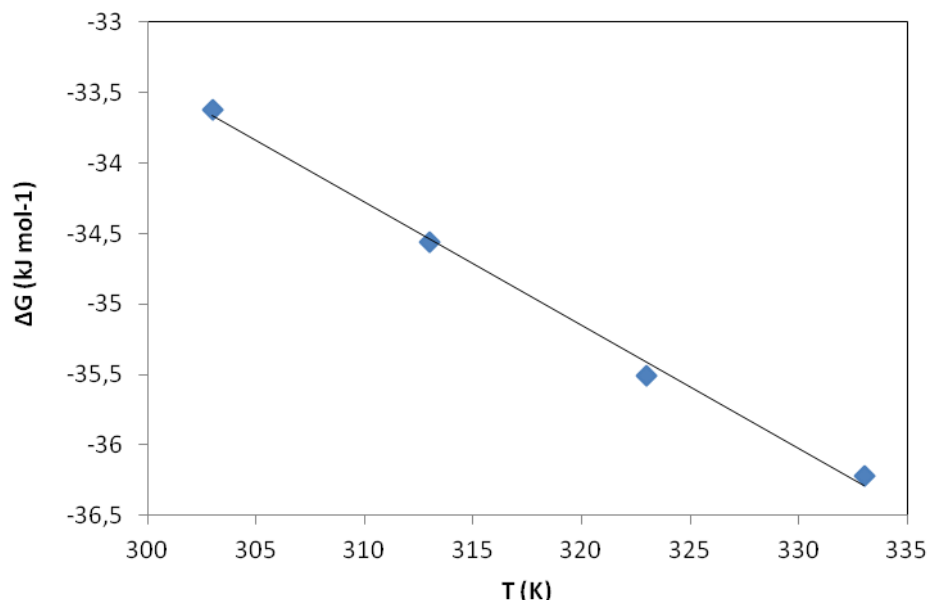


Figure 10. Plot of ΔG_{ads} versus absolute temperature.

The value of ΔS_{ads} is positive in the adsorption process and this could be explained as follows: The thermodynamic values obtained are the algebraic sum of the adsorption of organic molecules and desorption of water molecules [34]. Therefore, the gain in entropy is attributed to the increase in solvent entropy [34, 35]. The value of ΔH_{ads} provides further information about the mechanism of corrosion inhibition. The endothermic adsorption process is ascribed unambiguously to chemisorption and an exothermic adsorption process may involve either physisorption or chemisorption or a combination of both [36]. In the present study, the negative values of ΔH_{ads} obtained indicate a combination of both chemisorption and physisorption processes.

The values of ΔH_{ads} and ΔS_{ads} can also be calculated by using following equation:

$$\Delta G_{ads} = \Delta H_{ads} - T\Delta S_{ads} \quad (9)$$

Using Eq. (9), the plot of ΔG_{ads} versus T gives a straight line (Fig. 10) with a slope of $-\Delta S_{ads}$ and intercept of ΔH_{ads} . The values obtained are well correlated with those obtained from Eq. (8).

3.6. Synergetic effect

The corrosion of mild steel in 0.5 M HCl in the absence and presence of AB and AB in combination with KI was studied by gravimetric and electrochemical techniques at 30° C and the values are summarized in Table 5. The AB – KI combination produce pronounced effects on the anodic and cathodic currents density compared to those displayed by only AB, and shift of E_{corr} in the positive direction. Also, the rates of both anodic and cathodic reaction decreases substantially leads to higher inhibition efficiency of 96 %, compared to 76 % obtained for AB alone (Figs. 11 and 12).

Synergetic effects are also revealed in the impedance spectra obtained for mild steel in the inhibited solution.

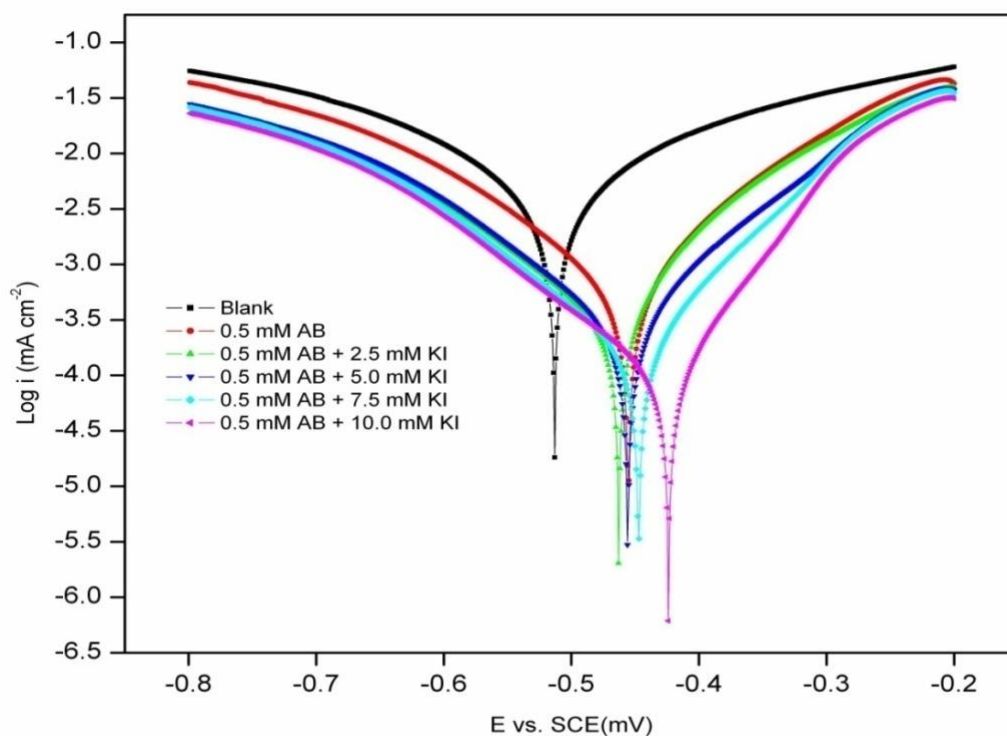


Figure 11. Polarization curves for mild steel in 0.5 M HCl containing different concentrations KI.

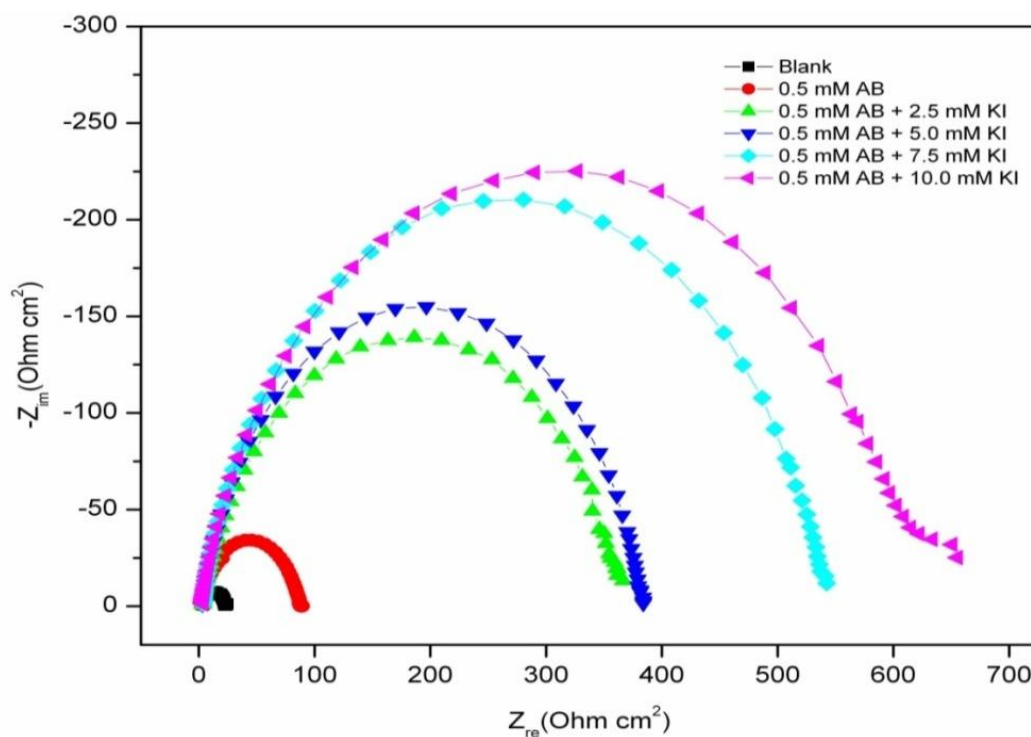


Figure 12. Nyquist plots for mild steel in 0.5 M HCl containing different concentrations KI.

Table 5. IE (%) obtained from weight loss, polarization and impedance measurements for mild steel in 0.5 M HCl containing various concentrations KI at 0.5 mM AB

C, mM	IE (%)		
	Weight Loss	Polarization	EIS
0.5	78.55	76.14	76.38
0.5 + 2.5 KI	90.52	92.32	92.63
0.5 + 5.0 KI	92.11	93.94	93.21
0.5 + 7.5 KI	95.40	97.21	96.90
0.5 +10.0 KI	96.12	98.87	99.25

The results illustrated in Fig. 12 showed that increase in the concentration of KI from 2.5 mM to 10 mM leads to increase in the diameter of semicircle in the Nyquist plot. These increases are again more substantial than those obtained for AB alone. The adsorption ability of halide ions on the metal surface is in the order $I^- > Br^- > Cl^-$ [37].

The greater influence of the iodide ion is attributed to its high hydrophobicity, large ionic radius and low electronegativity compared to other halide ions [38]. Halide ions are capable of increasing the adsorption of the organic cations by forming intermediate bridges between the positively charged metal surface and the positive end of the organic inhibitor.

The improved inhibition efficiency of AB in combination with halide ions is due to strong chemisorption of iodide ions on the metal surface [39, 40].

The cation is then adsorbed by coulombic attraction on the metal surface where iodide ions are already adsorbed by chemisorption. Stabilization of adsorbed iodide ions with cations leads to greater surface coverage and thereby greater inhibition. Similar observation has been reported by Larabi and Harek [41]

3.7. SEM studies

The surface morphology of the mild steel coupons was examined by scanning electron microscopy. SEM photographs of the polished mild steel surface (Fig. 13a) and mild steel surface without and with inhibitor (5 mM) in hydrochloric acid medium were obtained. The SEM photograph in the absence of AB shows cracks on the surface of the metal (Fig. 13b). But in the presence of AB, these are in better conditions having smooth surface compared with that of surface immersed in 0.5 M HCl alone (Fig. 13c). This is due to the formation of protective organic layer on the metal surface and the compound formed hinders the dissolution of iron [42].

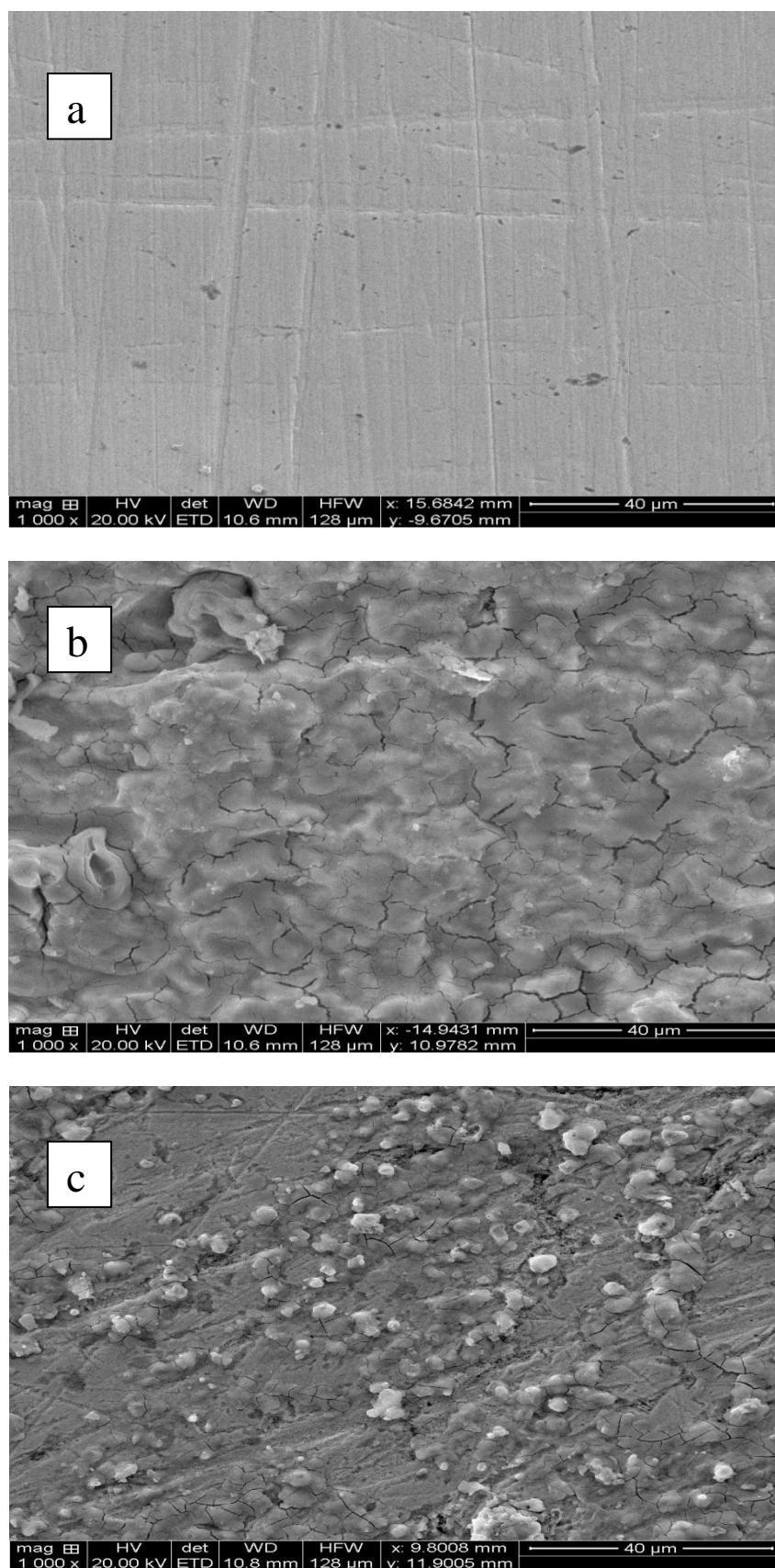


Figure 13. SEM images of mild steel in 0.5 M HCl solution after 6 h immersion at 30 °C (a) before immersion (polished) (b) After immersion without inhibitor (c) with 5 mM AB.

3.8. Quantum chemical calculations

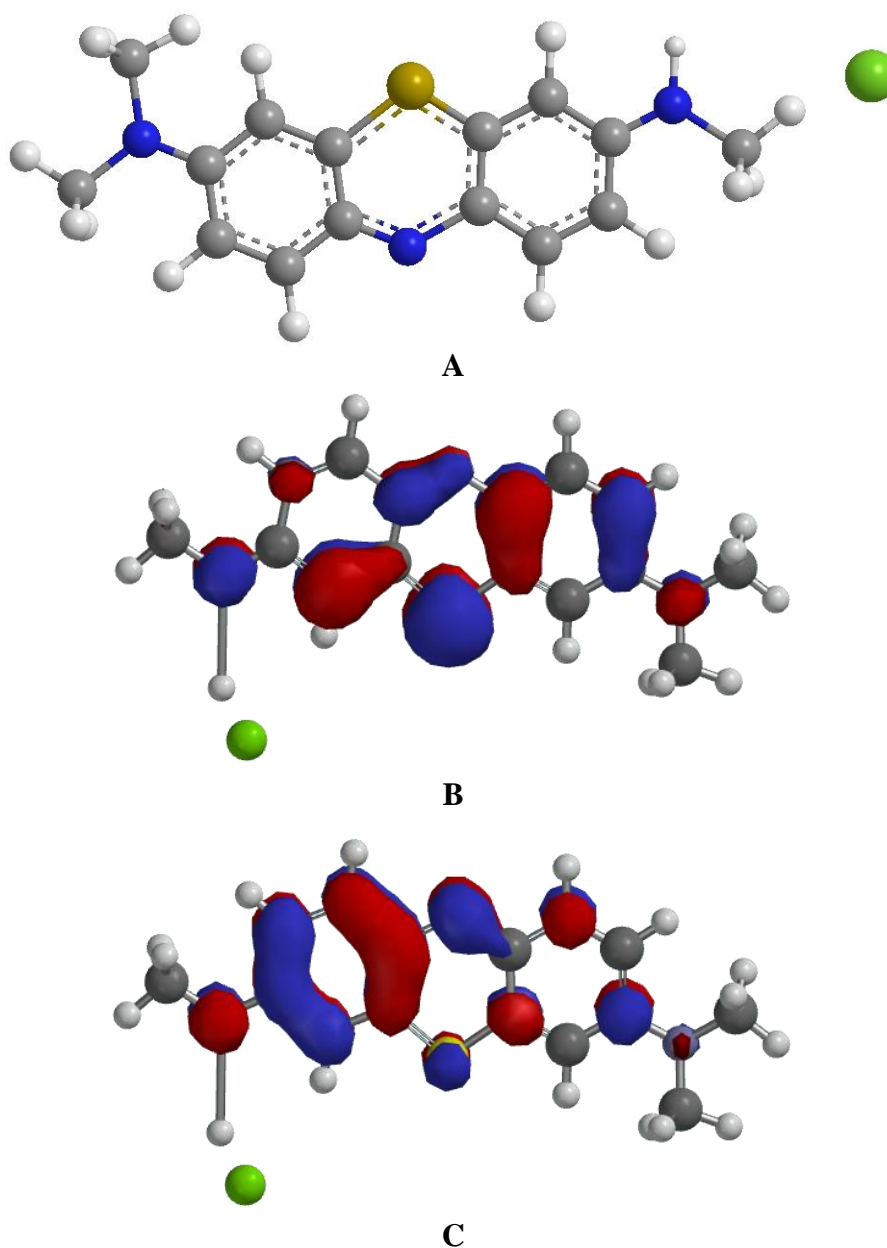


Figure 14. (a) Optimized structure, (b) HOMO and (c) LUMO of AB.

Quantum chemical study can be used as a strong tool to obtain information about the electronic interactions of inhibitor molecules with the metal surface and pre-selection of new inhibitors on the basis of empirical knowledge [43]. These facts have made quantum chemical calculations to be a very powerful tool for studying corrosion inhibition mechanism. Quantum chemical study has been performed by AM1 method using the Spartan 08 V1.2.0 semi-empirical program. Fig 14 shows optimized molecular structure, HOMO and LUMO of AB.

The quantum chemical parameters enable us to focus on some of the parameters that directly influence the electronic interaction of the inhibitor molecules with the metal surface. These are mainly

highest occupied (E_{HOMO}) and lowest unoccupied (E_{LUMO}) molecular orbitals, dipole moment (μ) and total energy (E_{tot}). The values of calculated quantum chemical parameters are listed in Table 6.

Table 6. Quantum chemical parameters for AB

μ (D)	E_{HOMO} (eV)	E_{LUMO} (eV)	$E_{LUMO-HOMO}$ (eV)	E_{tot} (kJ/mol)
3.76	-7.82	-1.32	6.50	372.86

These quantum chemical parameters were obtained after geometric optimization with respect to all nuclear coordinates. E_{HOMO} is related with the electron donating ability of the molecule and high E_{HOMO} values indicate that the molecule has a tendency to donate orbital electrons to an appropriate acceptor with empty molecular orbital and E_{LUMO} connected with the ability of the AB to accept electrons.

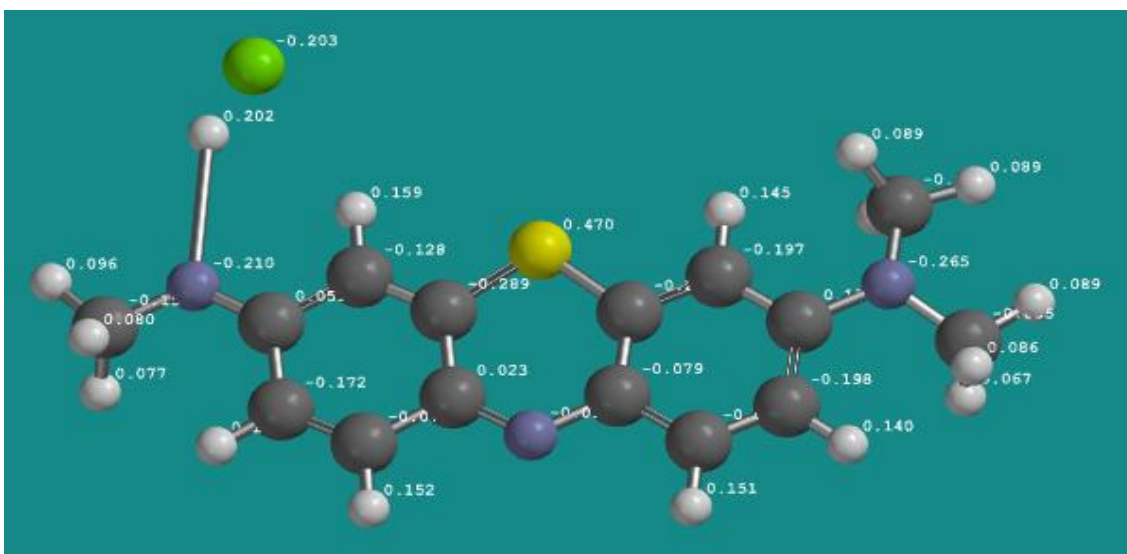


Figure 15. The Mulliken charge density of AB molecule.

The orbital with lower the value of E_{LUMO} , the more probable the molecule would accept electrons. In the same way, low values of the energy gap ($\Delta E = E_{LUMO} - E_{HOMO}$) will yield good inhibition efficiencies, because the energy required to remove an electron from the last occupied orbital will be low [44]. Similarly, low values of the dipole moment (μ) will favor the accumulation of inhibitor molecules on the metallic surface [45]. Reportedly, good corrosion inhibitors are usually those organic compounds which not only offer electrons to unoccupied orbital of the metal, but also accept free electrons from the metal [43, 46].

Figs. 14b and 14c show that the frontier orbital HOMO were distributed around the thiazin ring and benzene ring with dimethyl groups while the LUMO were mainly on the benzene ring which is attached to the methylamine group and carbon atoms which are adjacent to the nitrogen and sulphur

atom of the thiazin ring. The use of Mulliken population analyses to investigate the adsorption centers of inhibitors has been widely reported [47]. The Mulliken charge distribution of AB is presented in Fig. 15. It could be readily observed that nitrogen atoms and the benzene ring have higher charge densities and might form the adsorption centers. AB can interact with mild steel forming a good protective layer on the steel surface, thus retarding corrosion of the metal in hydrochloric acid solution.

4. CONCLUSIONS

- AB functions as an effective inhibitor for mild steel corrosion in 0.5 M HCl solution.
- Polarization curves indicated that AB behaves as mixed type of inhibitor.
- The adsorption of AB on the mild steel surface in 0.5 M HCl solution obeyed Langmuir adsorption isotherm.
- The inhibition efficiency was synergistically increased by the addition of KI.
- The calculated quantum chemical parameters such as E_{HOMO} and E_{LUMO} molecular orbitals, dipole moment (μ) and total energy (E_{tot}) support the inhibition mechanism of AB.

References

1. G.O. Avwiri and F.O. Igho, *Mater. Lett.* 57 (2003) 3705
2. E.E. Oguzie, *Corros. Sci.* 49 (2007) 1527
3. A. Popova, M. Christov, S. Raicheva and E. Sokolova, *Corros. Sci.* 46 (2004) 1333
4. N.A. Negm, Y.M. Elkholy, M.K. Zahran and S.M. Tawfik, *Corros. Sci.* 52 (2010) 3523
5. J. De Damborenea, J.M. Bastidas and A.J. Vazquez, *Electrochim. Acta.* 42 (1997) 455
6. S.S. Abd El Rehim, M.A.M. Ibrahim, and K.F. Khaled, *J. Appl. Electrochem.* 29 (1999) 593
7. N.A. Negm, Y.M. Elkholy, M.K. Zahran and S.M. Tawfik, *Corros. Sci.* 52 (2010) 3523
8. J. De Damborenea, J.M. Bastidas and A.J. Vazquez, *Electrochim. Acta.* 42 (1997) 455
9. R. Solmaz, G. Kardas, B. Yazici and M. Erbil, *Prot. Met.* 41 (2005) 581
10. G.N. Mu, X.M. Li and F. Li, *Mater. Chem. Phys.* 86 (2004) 59
11. F. Bentiss, M. Bouanis, B. Mernari, M. Traisnel and M. Lagrenee, *J. Appl. Electrochem.* 32 (2002) 671
12. E.E. Ebenso, *Mater. Chem. Phys.* 79 (2003) 58
13. D.D.N. Singh, T.B. Singh and B. Gaur, *Corros. Sci.* 37 (1995) 1005
14. M. Hosseini, S.F.L. Mertens, and M.R. Arshadi, *Corros. Sci.* 45 (2003) 1473
15. M. Abdeli, N.P. Ahmadi R.A and Khosroshahi, *J. Solid. State. Electrochem.* 14 (2010) 1317
16. A.I. Onen, O.N. Maitera, J. Joseph and E.E. Ebenso, *Int. J. Electrochem. Sci.* 6 (2011) 2884
17. E.E. Ebenso, H. Alemu, S.A. Umoren and I.B. Obot, *J. Electrochem. Sci.* 3 (2008) 1325
18. P. Raja and M. Sethuraman, *Mater. Lett.* 62 (2008) 1602
19. D. Gopi, K.M. Govindaraju and L. Kavitha, *J. Appl. Electrochem.* 40 (2010) 1349
20. F. Bentiss, M. Traisnel and M. Lagrenee, *Corros. Sci.* 42 (2000) 127
21. S. Murlidharan, K.L.N. Phani, S. Pitchumani and S. Ravichandran, *J. Electrochem. Soc.* 142 (1995) 1478
22. S.S. Abdel Rehim, O.A. Hazzazi, M.A. Amin and F.K. Khaled, *Corros. Sci.* 50 (2008) 2258
23. H. Ashassi Sorkhabi, D. Seifzadeh and M.G. Hosseini, *Corros. Sci.* 50 (2008) 3363

24. M. Schorr and J. Yahalom, *Corros. Sci.* 12 (1972) 867
25. L. Larabi, O. Benali and Y. Harek, *Mater. Lett.* 61 (2007) 3287
26. Y.K. Agrawal, J.D. Talati, M.D. Shah, M.N. Desai, N.K. Shah, I.K. Putilova, S.A. Balezin and Y.P. Barasanik, *Metallic Corrosion Inhibitors*. Pergamon Press, Oxford (1960)
27. M. Abdallah, *Corros. Sci.* 44 (2002) 717
28. E.A. Noor and A.H. Al-Moubaraki, *Mater. Chem. Phys.* 110 (2008) 145
29. S.S. Abd El-Rehim, S.A.M. Refaey, F. Taha, M.B. Saleh and R.A. Ahmed, *J. Appl. Electrochem.* 31 (2001) 429
30. M.A. Quraishi and S. Khan, *J. Appl. Electrochem.* 36 (2006) 539
31. E.S.M. Sherif, R.M. Erasmus and J.D. Comins, *J. Colloid. Interface. Sci.* 306 (2006) 96
32. S.A. Ali, M.T. Saeed, and S.U. Rahman, *Corros. Sci.* 45 (2003) 253
33. E. Bensajjay, S. Alehyen, M. El Achouri and S. Kertit, *Anti-Corros. Meth. Mater.* 50 (2003) 402
34. Emranuzzaman, T. Kumar, S. Vishwanatham and G. Udayabhanu, *Corros. Eng. Sci. Technol.* 39 (2004) 327
35. B. Ateya, B. El-Anadauli and F. El Nizamy, *Corros. Sci.* 24 (1984) 509
36. S.A. Ali, A.M. El Shareef, R.F. Al Ghamdi and M.T. Saeed, *Corros. Sci.* 47 (2005) 2659
37. G.K. Gomma, *Mater. Chem. Phys.* 55 (1998) 241
38. C. Jeyaprabha, S. Sathiyarayanan, S. Muralidharan and G Venkatachari, *J. Braz. Chem. Soc.* 17 (2006) 61
39. Z.S. Syed, S. Muralidharan, S. Venkatakrishna Iyer, B. Muralidharan and T. Vasudevan, *Brit. Corros. J.* 33 (1998) 297
40. S.H. Sanad, A.A. Ismail and N.A. Mahmoud, *J. Mater. Sci.* 27 (1992) 5706
41. L. Larabi, Y. Harek, M. Traisnel and A. Mansri, *J. Appl. Electrochem.* 34 (2004) 833
42. R.A. Prabhu, T.V. Venkatesha and A.V. Shanbhag, *J. Iran. Chem. Soc.* 6 (2009) (2) 353
43. L. Lukovits, E. Kalman and F. Zucchi, *Corrosion.* 57 (2001) 3
44. D.Q. Zhang, Z.X. An, Q.Y. Pan, L.X. Gao and G.D. Zhou, *Corros. Sci.* 48 (2006) 1437
45. J. Fang and J. Li, *J. Mol. Struct. (Theochem)* 593 (2002) 179
46. L.M. Rodrigues Valdez, W. Villamisar, M. Casales, J.G. Gonzalez Rodriguez, A. Martnez Villafane, L. Martinez and D. Glossman Mitnik. *Corros. Sci.* 48 (2006) 4053
47. N.K. Allam, *Appl. Surf. Sci.* 253 (2007) 4570